# The Role of Aerosol Absorption in Driving Solar Dimming

Geeta G. Persad,[1] Yi Ming,[2] V. Ramaswamy,[2]

Corresponding author: G.G. Persad, Program in Atmospheric and Oceanic Sciences, Princeton University, 201 Forrestal Road, Princeton, NJ 08540, USA. (gpersad@princeton.edu)

[1]Program in Atmospheric and Oceanic Sciences, Princeton University, Princeton, New Jersey, USA.

[2]Geophysical Fluid Dynamics Laboratory, Princeton/NOAA, New Jersey, USA.

**Abstract.**

Surface-based observations have indicated a significant decreasing trend in clear-sky surface solar radiation (SSR) over East Asia since the 1960s. This dimming is thought to be driven by the region's long-term increase in aerosol emissions, but little work has been done to quantify the underlying physical mechanisms or, more specifically, the contribution to the surface values from aerosol absorption within the atmospheric column. Given the distinct climate impacts that absorption-driven dimming may produce, this constitutes an important, but thus far neglected, line of inquiry.

We conduct experiments using two of the Geophysical Fluid Dynamics Laboratory's Atmospheric General Circulation Models, AM2.1 and AM3, in order to analyze the model-simulated East Asian SSR trends and to understand the aerosol-related mechanisms responsible. We also use the models' standalone radiation module to examine how various aerosol characteristics in the two models (such as burden, mixing state, hygroscopicity, and seasonal distribution) contribute to the trends produced. Both models produce trends in clear-sky SSR that are comparable to that observed, but via very different mechanisms. Surprisingly, despite their different aerosol treatments, the models produce nearly identical increases in aerosol absorption since the 1960s that constitute as much as half of the dimming. We find that this is due to a compensation between the aerosol column burden and mixing state differences in the two models, i.e. plausible SSR simulations can be achieved via drastically different physical realizations of aerosols. Our novel results

suggest that absorption drives a large portion of East Asian dimming, and that a mechanistic analysis of the absorption contribution to dimming is an important diagnostic that models should implement when evaluating their aerosol formulation.

## 1. Introduction

Surface solar radiation (SSR) governs the energy available for both sensible and latent heat release, with significant implications for the hydrological cycle and convection [*Ramanathan et al.*, 2001; *Andrews et al.*, 2009]. Studies of surface-based observations dating back to the 1950s, however, indicate that there have been decadal variations in the amount of solar radiation reaching the Earth's surface [*Wild*, 2009, and references therein]. Observation sites world-wide experienced a decrease in SSR from the 1950s to the 1980s, followed by an increase in the following decades in certain regions such as Europe and North America. The observed surface trends are an order of magnitude larger than observed variations in top-of-atmosphere insolation [*Fröhlich and Lean*, 1998; *Willson and Mordvinov*, 2003] and are evident under both all-sky and clear-sky conditions [*Wild*, 2009].

In the case of clear-sky SSR, possible trend explanations focus on changes in atmospheric composition. Radiative transfer calculations indicate that changes in water vapor much larger than those observed would be necessary to effect the observed SSR changes [*Wild*, 1997]. This leaves changes in aerosol concentrations as the most plausible explanation for clear-sky SSR variability. Aerosols can attenuate shortwave radiation by either scattering or absorbing it, reducing the amount that reaches the surface. A number of studies have strongly correlated decadal changes in aerosol emissions with decadal changes in SSR, particularly on a regional scale [*Streets et al.*, 2006, 2009; *Freidenreich and Ramaswamy*, 2011]. Modeling studies (including the results of this work) support a causal relationship between aerosol and SSR changes, indicating that increasing aerosol concentrations can

drive large regional decreases in SSR [e.g. *Nazarenko and Menon*, 2005; *Ramanathan et al.*, 2005; *Freidenreich and Ramaswamy*, 2011].

Over Asia, in particular, trends in SSR have manifested largely as a decrease throughout the observational record. A synthesis of observational studies over China suggests a decreasing trend in all-sky SSR of approximately 7 $\mathrm{Wm^{-2}decade^{-1}}$ during the 1950s-1980s [*Wild*, 2012]. This "dimming," as it is colloquially known, has been strongly correlated with increasing emissions of sulfate and black carbon aerosols regionally [*Che et al.*, 2005; *Qian et al.*, 2006, 2007]. China, therefore, constitutes an ideal location over which to analyze aerosols' interaction with shortwave radiation and ways in which this interaction may impact SSR values. We, thus, focus our analysis on this region.

Whether an aerosol-driven decrease in SSR comes primarily from increased scattering or from increased absorption can have a significant impact on how the regional climate responds to the SSR perturbation. Absorption traps radiative energy within the atmosphere, while scattering reflects that energy back out of the surface/atmosphere system. As discussed by *Ramanathan and Carmichael* [2008], surface cooling associated with an SSR reduction, coupled with atmospheric heating from aerosol absorption within the atmospheric column, can weaken the radiative-convective coupling of the atmosphere and decrease evaporation and precipitation. *Ming et al.* [2010], meanwhile, demonstrated that atmospheric heating by absorbing aerosols can have an effect on precipitation that counteracts and even outweighs the aerosols' TOA forcing.

Few existing papers, however, analyze the contribution of aerosols to clear-sky SSR variations in particular [*Wild*, 2009], and fewer yet have analyzed the relative contributions of absorption and scattering in model simulations. Several studies have compared modeled

clear-sky SSR with observed clear-sky proxy data [e.g. *Norris and Wild*, 2007, 2009; *Ruckstuhl and Norris*, 2009; *Dwyer et al.*, 2010; *Allen et al.*, 2013], but these studies focus on model trend intercomparison rather than on detailed analysis of the mechanisms behind the modeled trends or the robustness thereof.

In the few studies in which the scattering and absorption contributions to dimming trends have been distinguished, the mechanisms responsible for the modeled scattering and absorption are not elucidated [e.g. *Folini and Wild*, 2011]. *Stier et al.* [2007] identify that subtle variations in the microphysics of the aerosol representation can significantly affect the modeled amount of absorption and overall shortwave attenuation. Given the myriad climate impacts of aerosol absorption, an in-depth analysis of how much absorption models produce and via what particular mechanisms will be vital to a full picture of how the climate will respond to changes in SSR.

This study seeks to advance the existing literature through a detailed analysis of the relative contributions of aerosol scattering and absorption to modeled clear-sky SSR trends over China, the mechanisms responsible for the simulated absorption, and the sensitivity of that absorption to variations in characteristics of the aerosol treatment. We achieve this using a model hierarchy that allows us to analyze from the large-scale trend down to the aerosol microphysics responsible. We use ensemble simulations in the Geophysical Fluid Dynamics Laboratory's (GFDL) AM2.1 and AM3 atmospheric general circulation models (AGCMs)—included in the CMIP3 and CMIP5 multi-model data archives, respectively—to isolate the impact of aerosols on the dimming trends, and analyze output shortwave radiation variables to characterize the contribution from atmospheric absorption. We then use each model's standalone radiation module, which allows manipulation of the aerosol

treatment, to quantify how various aerosol characteristics (including aerosol burden, mixing state, and hygroscopic growth) contribute to the dimming and absorption. Our goal is both to understand the aerosol mechanisms driving the observed clear-sky trends in SSR over China and to explore the sensitivity to the models' aerosol treatment.

We focus our analysis primarily on the effects of sulfate and black carbon aerosols on clear-sky dimming. Sulfate aerosol from the oxidation of sulfur dioxide emissions is considered to be the most potent anthropogenic scatterer [*Charlson et al.*, 1991], while black carbon aerosol from incomplete combustion processes is considered to be the most potent anthropogenic absorber [e.g. *Jacobson*, 2000; *Sato et al.*, 2003]. Aerosols can also modify the shortwave radiation budget via their impact on clouds [e.g. *Twomey*, 1974; *Kaufman*, 1997; *Ackerman*, 2000; *Lohmann and Feichter*, 2001]. However, significant uncertainty is associated with these indirect effects and their representation in models, especially regarding the effect of aerosol absorption on clouds [e.g. *Koch and Del Genio*, 2010; *Persad et al.*, 2012; *Bond et al.*, 2013]. We, therefore, concentrate solely on issues surrounding the simulation of the clear-sky effects of these two major aerosol species.

Our results demonstrate the importance of aerosol absorption in driving solar dimming over China and the contribution to that absorption from different characteristics of the models' aerosol treatment. This study constitutes the first time, to our knowledge, that the absorption contribution to regional dimming in models has been mechanistically analyzed. The outcomes detailed here suggest that this is an important diagnostic that models should implement when evaluating their aerosol formulation.

## 2. Methods

### 2.1. Model description

Using GFDL's AM2.1 and AM3 AGCMs, we simulate the trends in SSR over China from 1960 through the mid-2000s (the period covered by many observational studies). The two models are the atmospheric components of the fully coupled atmosphere-ocean GCMs included in the CMIP3 and CMIP5 model archives (GFDL-CM2.1 and GFDL-CM3, respectively). These two models produce credible simulations of the important role of aerosols in offsetting historic greenhouse gas warming and highlight the global and regional role of aerosols in 20th century temperature evolution [*The GFDL Global Atmospheric Model Development Team (GAMDT)*, 2004; *Reichler and Kim*, 2008; *Donner et al.*, 2011; *Klein et al.*, 2013], and are thus excellent tools for studying aerosols' radiative effects.

The AM2.1 and AM3 aerosol treatments contain several differences (summarized in Table 1), many of which are typical of improvements made between the CMIP3 and CMIP5 generations of climate models. Generally, advances in computing resources and theoretical understanding have allowed for more complex treatment of aerosols in the newer models [*Donner et al.*, 2011]. Full descriptions of the two models can be found in *The GFDL Global Atmospheric Model Development Team (GAMDT)* [2004] and *Donner et al.* [2011], respectively, but aspects of the models' aerosol treatment salient to this investigation are summarized here.

Aerosol concentrations in AM2.1 are prescribed from off-line calculations with the MOZART chemistry transport model [*Horowitz et al.*, 2003] using emissions from *Olivier* [1996] and *Cooke et al.* [1999] with optical properties described by *Haywood et al.* [1999]

and *Haywood and Ramaswamy* [1998]. Once input into AM2.1, these prescribed concentrations can radiatively impact the model meteorology, but are not transported or removed by that meteorology. As such, the meteorological fields used by MOZART to produce the aerosol concentrations seen by AM2.1 are not consistent with the meteorological fields produced by AM2.1 itself. Sulfate, black carbon, organic carbon, sea salt and dust aerosol species are considered. All aerosol types are treated as externally mixed, i.e. though a given aerosol population may contain many different species, any individual aerosol particle is composed purely of one species. Sulfate is treated as hydrophilic, while black carbon is treated as hydrophobic. Hygroscopic growth of sulfate aerosol continues through 100% relative humidity.

Aerosol concentrations in AM3, conversely, are interactive with AM3's meteorology. Anthropogenic sulfate, black carbon, and organic carbon emissions from *Lamarque et al.* [2010] are input into AM3 and are transported, aged, and removed according to the meteorology and chemistry within the model itself. Other natural and anthropogenic aerosol species (including sea salt, secondary organic aerosols, and dust) are similarly interactive in the model. Sulfate and black carbon aerosols are assumed to be internally mixed in the model, i.e. coexisting sulfate and black carbon will mix with each other at the individual particle level. The refractive index of the sulfate/black carbon mixture is calculated in the model as a volume-weighted average of the refractive indices of each aerosol species. Black carbon, although largely hydrophobic on its own, will grow hygroscopically when internally mixed with sulfate. Hygroscopic growth is capped at 97% relative humidity in AM3. Organic carbon contains slight absorption in AM3's formulation [*Donner et al.*, 2011], but this absorption is minor compared to that of black carbon [*Ocko et al.*, 2012].

The optical properties of other aerosol species, which remain externally mixed, are identical to those used in AM2.1. The simulation and effects of dust also remain identical between the two models and do not contribute to model differences.

### 2.2. Design of experiments

We perform a set of four historical (1861-2003 in AM2.1 and 1870-2005 in AM3) AGCM simulations in order to isolate the contribution of anthropogenic aerosols to the modeled trend in clear-sky SSR over China: (1) A five-member ensemble of experiments that include all forcings (ALL_F), including anthropogenic (aerosols, greenhouse gasses, and land-use changes) and natural (solar variations and volcanoes) forcings; (2) A three-member ensemble containing only anthropogenic aerosol forcing (AERO); (3) A three-member ensemble containing only anthropogenic well-mixed greenhouse gas and ozone forcings (WMGG); (4) A three-member ensemble containing only natural forcings (NAT). All results shown in this paper are ensemble averages. These simulations are forced with the observed historical sea surface temperatures and sea ice. They have been further described in *Bollasina et al.* [2011].

### 2.3. Standalone radiative transfer calculation

The radiative transfer modules of AM2.1 and AM3 can be run in a standalone mode, independent of the full models, to produce shortwave and longwave fluxes for a set of atmospheric conditions (e.g. temperature, water vapor, clouds, greenhouse gas and aerosol concentrations, and surface albedo). These conditions are saved from an interactive GCM integration (here, an AM3 all-forcing simulation). These input data can be modified to substitute one aerosol climatology for another, to change the mixing state of the aerosol

population, and to turn on and off the radiative effects of microphysical processes like hygroscopic growth.

We utilize this capability to test the influence of various aspects of the aerosol radiative properties on the model-simulated dimming and absorption. We perform the following standalone radiative transfer perturbation experiments over one model year: (1) a control case in which the default AM2.1 and AM3 settings are used (AM2_EM and AM3_IM, respectively, with EM denoting external mixing and IM denoting internal mixing), (2) switched mixing state, i.e. AM2.1's aerosol climatology with internal mixing and AM3's aerosol climatology with external mixing (AM2_IM and AM3_EM, respectively), (3) hygroscopic growth turned off (..._nohygro), (4) aerosol radiative effects turned off (..._noaero). These experiments are performed for 1970 and 1990 aerosol burdens in each model. These years are those closest to the endpoints of the relevant time period for which aerosol concentrations are provided in both models. All other atmospheric and surface constituents are held constant, including surface albedo. The values shown in this paper are for 1990 aerosol runs minus 1970 aerosol runs to provide trend-relevant results.

### 2.4. Observational context

An often-used dataset for comparison of modeled and observed dimming over East Asia is that originally published by *Norris and Wild* [2009]. It is compared with CMIP3 models in *Dwyer et al.* [2010] and with CMIP5 models in *Allen et al.* [2013]. Monthly mean anomalies in all-sky SSR over China are computed from measurements made at surface pyranometer sites in the Global Energy Balance Archive (GEBA). Clear-sky SSR values can then be derived by subtracting cloud effects from the all-sky values. *Allen et al.* [2013] used cloud observations from the International Satellite Cloud Climatology Project

(ISCCP) and visual cloud observation sources to perform quality control on the surface observation sites and to calculate a shortwave "cloud cover radiative effect anomaly" (CCRE′), which seeks to quantify the shortwave radiative impact of cloud cover anomalies. A time series of clear-sky SSR anomalies can then be extracted from the observed all-sky SSR anomalies by subtracting CCRE′ from the all-sky observations using linear regression. The resulting clear-sky SSR proxy anomalies produce a decreasing trend in clear-sky SSR over China of $-0.43 \pm 0.10$ $\mathrm{Wm^{-2}yr^{-1}}$ over the period from 1961-2007 [*Allen et al.*, 2013].

There are identified deficiencies in SSR datasets over China [*Shi et al.*, 2008; *Tang et al.*, 2010, 2011]. The clear-sky SSR proxy anomalies can be split into a "dimming" period from 1961-1989 and "brightening" period from 1990-2007, divided by a minimum in the data in 1990 [*Allen et al.*, 2013]. However, *Tang et al.* [2011] suggest that the minimum in 1990 and following increase in the early 1990s may be a spurious result of instrument retrofits that occurred during that period. We thus choose to focus on the linear trend in clear-sky proxy SSR over the entire time series to minimize possible biases caused by this suspect data.

## 3. Results

We analyze the SSR and atmospheric absorption anomalies over the eastern portion of China (22.5°-40° N and 100°-122.5° E) during the period 1960-2005 for AM3 and 1960-2003 for AM2.1, consistent with the spatial and temporal coverage of the *Norris and Wild* [2009] dataset. Observational estimates of clear-sky SSR are characterized by strong interannual and multidecadal variability, while the model variability is much smaller on both timescales (Figure 1). Although observations are for a single realization of the climate system while the model results are ensemble mean, individual model ensemble

members do not exhibit large variability either, indicating that ensemble averaging does not explain the difference in variability between the models and observations. A more likely cause is the low temporal resolution of the aerosol climatologies used in the models, as will be discussed in Section 4.

Over the entire time period, AM2.1 and AM3 have linear trends of $-0.47 \pm 0.02$ $\mathrm{Wm^{-2}yr^{-1}}$ and $-0.30 \pm 0.02$ $\mathrm{Wm^{-2}yr^{-1}}$, respectively. These values are both comparable to the $-0.43 \pm 0.10$ $\mathrm{Wm^{-2}yr^{-1}}$ trend seen in *Allen et al.* [2013]; AM2.1 is within the uncertainty of the observational dataset, and AM3's 95% confidence interval is just outside that of the observations. Despite significantly different aerosol treatments, as mentioned above, both models have been acknowledged to outperform others in their respective model generations in capturing the observed trend over Asia [*Dwyer et al.*, 2010; *Allen et al.*, 2013],

A natural next question is, what is the primary driver of the trends in SSR over China produced by the models? Figures 2 and 3 show the results of the various ensemble simulations (described in Section 2.1) for the two models. The natural forcing runs (NAT) shows no significant trend in clear-sky SSR, nor do the WMGG runs. The AERO run, meanwhile, produces a trend in SSR of $-0.23$ $\mathrm{Wm^{-2}yr^{-1}}$ in AM3 and $-0.49$ $\mathrm{Wm^{-2}yr^{-1}}$ in AM2.1, demonstrating that anthropogenic aerosols are indeed responsible for the majority of the all-forcing clear-sky SSR trends in both models, as previously postulated by many other studies [*Wild*, 2012, and references therein].

Both aerosol-induced scattering and absorption give rise to the reduction in SSR (Figures 4 and 5). Somewhat surprisingly, the two models produce almost identical increases in absorption ($\sim 0.16$ $\mathrm{Wm^{-2}yr^{-1}}$), despite the many differences in their aerosol formula-

tions. Since the overall reduction in SSR is larger in AM2.1 than in AM3, the fractional contribution from absorption is smaller in AM2.1 (about one third) than in AM3 (about one half). This indicates that rather strong absorption is crucial for both models to simulate a SSR trend that is reasonably close to the range of observations.

The models' standalone radiative transfer calculation allows for a process-level analysis of the contribution of various aerosol characteristics to the modeled SSR and absorption changes between 1970 and 1990. The key results are shown in Table 2. AM3's baseline configuration (AM3_IM) produces an annual mean surface solar radiation decrease between 1970 and 1990 of 6.9 $Wm^{-2}$ for AM3's aerosol concentrations, with an associated increase in atmospheric absorption of 4.3 $Wm^{-2}$. When external (AM3_EM) rather than internal mixing is used, however, the SSR decrease is only 5.6 $Wm^{-2}$ and the absorption increase is only 2.9 $Wm^{-2}$. The difference in the absorption increase (1.4 $Wm^{-2}$) is only slightly larger than the difference in the SSR decrease (1.3 $Wm^{-2}$), indicating that the increase in scattering from 1970 to 1990 is a relatively minor 0.1 $Wm^{-2}$ less with internal mixing than with external mixing.

AM2.1's baseline configuration (AM2_EM), meanwhile, produces an annual mean SSR decrease between 1970 and 1990 of 8.5 $Wm^{-2}$ with an associated increase in atmospheric absorption of 3.1 $Wm^{-2}$. When internal (AM2_IM) rather than external mixing is used, the SSR reduction increases to 10.3 $Wm^{-2}$ and the absorption increase rises to 6.5 $Wm^{-2}$. The SSR reduction increase (1.8 $Wm^{-2}$) is smaller than the rise in increased absorption (3.4 $Wm^{-2}$), again indicating that increased scattering between 1970 and 1990 is reduced (by $\sim$1.6 $Wm^{-2}$) when internal rather than external mixing is used. This suggests that

internal mixing promotes aerosol absorption while suppressing aerosol scattering in the models' radiative transfer calculations.

Increased absorption with internal mixing can be explained by the nonlinear relationship between the single scattering albedo of an internally mixed aerosol and its black carbon volume fraction [e.g. *Ackerman and Toon*, 1981; *Chylek and Wong*, 1995; *Jacobson et al.*, 2001; *Liao and Seinfeld*, 2005; *Stier et al.*, 2007]. As sulfate volume fraction decreases (i.e. as black carbon volume fraction increases) in the mixed aerosol, single scattering albedo decreases nonlinearly. For the large sulfate to black carbon volume ratios typical of most regions, a 0.1 decrease in sulfate fraction results in a single scattering albedo decrease of more than 0.1. This suggests that the amount of absorption produced by an aerosol population will be strongly sensitive to even small concentrations of black carbon when internal mixing is represented [e.g. *Ackerman and Toon*, 1981].

The absolute change in both SSR decrease and absorption increase between mixing states is much larger when using AM2.1's aerosol climatology than when using AM3's aerosol climatology. For example, the difference between AM2_IM and AM2_EM absorption is $\sim$3.3 $\mathrm{Wm}^{-2}$, while it is only $\sim$1.9 $\mathrm{Wm}^{-2}$ between AM3_IM and AM3_EM. Strikingly, AM2.1 sees almost twice as large of an increase in sulfate and black carbon column burden between 1970 and 1990 as AM3 does (1.24 $\times 10^{-5}$ kg $\mathrm{m}^{-2}$ versus 6.37 $\times 10^{-6}$ kg $\mathrm{m}^{-2}$ of sulfate, respectively, and 8.99 $\times 10^{-7}$ kg $\mathrm{m}^{-2}$ versus 5.41 $\times 10^{-7}$ kg $\mathrm{m}^{-2}$ of black carbon, respectively). This suggests that the difference between the two models' sensitivity to change in mixing state can be explained largely by the difference in aerosol column burden between the two models. Further confirmation of this result and consideration of its implications are presented in Section 4.

We also conduct standalone radiative transfer calculations for all previously discussed configurations with hygroscopic growth disabled (i.e. the optical properties of an aerosol is held constant at all relative humidities), the results of which are shown in Table 2. Note that the AM3 runs contain the 97% relative humidity cap described in Section 2.1, while there is no capping when AM2.1's aerosol climatology is used. We do not investigate the impact of the use of relative humidity capping on the modeled radiation, though it may be nonnegligible [*Ginoux et al.*, 2006].

In both models, with either mixing state implemented, disabling hygroscopic growth decreases the SSR reduction between 1970 and 1990. The degree to which this decreased dimming comes from decreased absorption versus decreased scattering, though, seems to depend on the mixing state. In the externally mixed case, the modeled absorption increase between 1970 and 1990 seems to be relatively insensitive to whether or not hygroscopic growth is disabled. However, with internal mixing, both models absorb more when hygroscopic growth is enabled. Additionally, the decrease in dimming due to disabled hygroscopic growth is larger than the decrease in absorption even in the internally mixed case, indicating that disabling hygroscopic growth also reduces scattering.

Why does hygroscopic growth only result in more absorption if internal mixing is implemented? Hygroscopic growth of an aerosol will increase the radiation incident on the aerosol due to the focusing effects of the dielectric medium (i.e. the liquid water) [e.g *Danielson et al.*, 1969]. When the aerosol is an absorber, hygroscopic growth can significantly increase its absorption cross-section [e.g. *Chylek et al.*, 1984; *Chylek and Wong*, 1995]. Absorbing black carbon only grows hygroscopically in the model when internally mixed with hydrophilic sulfate, and will thus only produce increased absorption from di-

electric focusing (represented in the model by an effective refractive index approximation) in the presence of internal mixing.

## 4. Discussion

### 4.1. Compensation between aerosol amount and mixing state

The sensitivity of the models' SSR and absorption to the mixing state of the aerosol provides a possible explanation for the similarity in the absorption increase that the models produce, despite significant differences in aerosol treatment. Although the change in mixing state, from external to internal, that occurred in the transition from AM2.1 to AM3 tends to increase absorption and decrease SSR, the change in aerosol column burdens operates in the opposite direction. This is evinced by the fact that when AM3's aerosol climatology is run with external mixing, it produces a much weaker signal than AM2.1's (Table 2). Indeed, as discussed in Section 3, AM2.1 contains an approximately twice as large increase in both types of aerosol between 1970 and 1990. This suggests a compensation of effects between aerosol amount and aerosol mixing state that may at least partially explain the similarity in the models' absorption trends.

This compensation can be probed quantitatively by calculating the absorption per unit aerosol produced by each model. If this value, which we term *normalized absorption*, converges for the two models when they are run in the same mixing state compared to the normalized value in different mixing states, we can argue that there is a compensation between aerosol amount and mixing state in the two models. The normalized absorption can be calculated as in the schematic equation (1) below. The absorptions (Abs) with (aero) and without (no_aero) aerosol are calculated by turning aerosol shortwave effects

on and off, respectively, in the standalone radiation code, and $\Delta$ refers to the change over the time period 1970-1990.

$$\textbf{Normalized Abs.} = \frac{\Delta \textbf{Abs}_{\text{aero}} - \Delta \textbf{Abs}_{\text{no\_aero}}}{\Delta \textbf{BC column burden}} \quad (1)$$

The results of this calculation are shown in Table 2. From the normalized absorption values, it is clear that the absorption converges when the effects of aerosol amount and mixing state are both accounted for. Although the baseline absorption values in each model are similar, they diverge when normalized for differences in aerosol amount but maintained in their differing baseline mixing states. However, when run in the same mixing state, the normalized absorption values again converge, indicating that the effects of the aerosol amount and mixing state changes mask each other in the base state of the models.

### 4.2. Potential effects of seasonality in aerosol amount

The standalone radiative transfer calculations analyzed here provide useful mechanistic insight into the impact of mixing state and hygroscopic growth treatment in aerosol schemes, but the framework developed in this study allows analysis of many other aerosol characteristics, e.g. the impact of the models' seasonal cycle of aerosol concentrations on their annual mean shortwave radiative effects. One might expect the annual mean SSR reduction or shortwave absorption induced by an aerosol population to be dependent on how well the seasonal distribution of aerosol correlates with the seasonal distribution of TOA shortwave radiation availability (i.e. insolation). One might also expect this effect to be present in diurnal averaging [e.g. *Kassianov et al.*, 2013].

The models have different seasonal concentrations in aerosol (due to the distinct emissions inventories and interactivity of aerosols), which have different temporal correlation with the seasonal TOA insolation distribution (Figure 6). We can hypothesize an expected annual mean sensitivity to this correlation using a simplistic calculation. The ability of a given seasonal distribution of black carbon over East China to interact with solar radiation can be calculated by comparing an annual area-averaged BC concentration ($BC'$) that has been weighted by the area-averaged seasonal insolation ($S$) with an unweighted concentration ($BC$). This provides a dimensionless, ordinal measure of the "potency" ($\Pi$) of a given aerosol seasonality at interacting with shortwave radiation in the annual mean. The calculation is as follows for monthly values, $t = \{1, 2, 3, \ldots, 12\}$:

$$BC' = \frac{\sum_{t=1}^{12} BC(t) \times S(t)}{\sum_{t=1}^{12} S(t)} \qquad \rightarrow \qquad \Pi = \frac{BC'}{BC} \tag{2}$$

This potency value ($\Pi$) can be used for first-order comparison of the impact of the seasonal aerosol distribution on the annual mean shortwave values in each model. A larger potency suggests stronger interaction between the BC concentration and insolation. The calculated potency values for AM2.1 and AM3 are 0.086 and 0.084, respectively.

The similarity of these values suggests that the difference in the models' seasonal distribution has minimal impact on the annual mean values produced. More analysis via standalone radiation transfer calculations would be needed, however, to confirm this behavior.

### 4.3. Evaluation of aerosol treatments

The results of this study suggest that both AM2.1 and AM3 are capable of producing trends in SSR comparable with observational estimates, but that the aerosol processes responsible are quite different. Given this dichotomy, which model's aerosol configuration is more physical? Answering this question is vital for improved aerosol modeling, but is made less tractable by persistent uncertainty in many aerosol processes and in aerosol emissions, partially driven by a lack of aerosol observations that are both global and detailed [*Koch et al.*, 2009; *Bond et al.*, 2013]. We nonetheless attempt to comment on the relative physicality of various relevant aspects of the two models' aerosol treatment.

Both modeling and observational studies have found that the majority of aerosol populations will be largely internally mixed after aging [e.g. *Andreae et al.*, 1986; *Pósfai et al.*, 1999; *Jacobson et al.*, 2001]. The representation of the internal mixture, however, can significantly impact the aerosols' radiative perturbation; *Jacobson* [2000] found a more than 40% increase in global direct radiative forcing from black carbon when a uniform mixing representation (like that in AM3) was used versus a coated core representation. The insolubility of black carbon likely makes a uniformly mixed mode (in which the sulfate and black carbon have diffused into a homogeneous aerosol) unphysical, though.

The way in which AM3 represents internal mixing may bias it toward a more pronounced absorption increase with internal mixing than is realistic. Comparisons between observations and the CMIP3-generation aerosol models (including AM2.1), however, indicate that those models underestimated BC absorption [*Koch et al.*, 2009]. *Bond et al.* [2013] also suggest that many current generation models underestimate black carbon absorption by a factor of three even when emissions biases are accounted for, suggesting that AM3's

strong absorption per unit black carbon may be warranted by observational estimates. Analyzing the relative contributions of diffuse and direct shortwave flux at the surface in models versus observations, as done by *Freidenreich and Ramaswamy* [2011], may provide one means of further constraining realistic absorption.

AM2.1's surface aerosol concentrations are lower than observations, but within a factor of two [*Ginoux et al.*, 2006]. However, it is important to note that surface concentration comparisons may not be transferrable to column burden, which is more relevant for total shortwave attenuation. AM2.1 is known to have an overly diffuse aerosol column over East China [*Koffi et al.*, 2012], which would prime the model to underestimate surface concentration while still maintaining a representative or even overestimated column burden. The literature is largely inconclusive on model over- or underestimation of aerosol concentrations over East Asia, partially because of challenges associated with difficult-to-track regional sources. Small but strongly emitting Asian industries, like brick kilns and coking, are often not included in bottom-up emissions inventories, making Asia particularly prone to emissions underestimations. *Bond et al.* [2013] suggest, nonetheless, that up to a factor of 4 increase in black carbon burdens over those found in current models may be warranted.

It is unclear to what extent the large difference in both sulfate and black carbon column burden between AM2.1 and AM3 over East Asia is a result of the different emissions inventories used versus differences in the model physics. There are larger global-mean black carbon emissions in AM2.1/MOZART than in AM3 (11 $\mathrm{Tgyr}^{-1}$ and 8.2 $\mathrm{Tgyr}^{-1}$, respectively) [*Donner et al.*, 2011], but this emissions difference does not entirely explain

the discrepancy in aerosol burden. Rates of dry and wet deposition of aerosol in the two models may also contribute and may need to be better constrained.

### 4.4. Limitations of observational comparison

Although these results suggest that AM3's more complex aerosol treatment constitutes an improvement over earlier formulations, further advances in aerosol representations in GCMs will require better field measurements against which to validate them [*Ginoux et al.*, 2006; *Bond et al.*, 2013]. *Allen et al.* [2013] and *Ruckstuhl and Norris* [2009], among others, showed that differences in the historical aerosol emissions used in models cannot by itself explain divergences in dimming trends; significant divergence in aerosol physics remains in the absence of sufficient observations for validation [*Koch et al.*, 2009]. As evinced by the results of this study, observations of aerosol radiative effects alone are not sufficient to constrain aerosol physics, as multiple realizations can produce plausible values.

While observational datasets provide useful context for model simulation, considerable uncertainty in both models and observations obfuscates direct model/observation comparison. For instance, many studies have analyzed the lack of interdecadal variability in modeled SSR, compared to observations [e.g. *Ruckstuhl and Norris*, 2009; *Dwyer et al.*, 2010; *Wild and Schmucki*, 2010; *Allen et al.*, 2013]. This should perhaps be unsurprising, however, given the low temporal resolution of models' aerosol climatologies. In AM2.1, monthly mean aerosol concentrations are only input from MOZART calculations every ten years. Aerosol concentrations between those calculated values are estimated by linear interpolation [*Ginoux et al.*, 2006]. AM3's aerosol emissions are, likewise, only input directly from the emissions inventory at approximately decadal intervals, with linear interpolation

in between. This linear interpolation and coarse temporal resolution will significantly damp variability of aerosol-driven values in the models.

In addition to the identified observational deficiencies discussed in Section 2.4, other issues favor focusing on model simulation rather than model/observation comparison. While *Allen et al.* [2013] are conscientious in applying the stringent quality standards needed to avoid contamination by possible system deficiencies, this leaves them with only six observation sites. *Wild* [2009] highlights that small sample sizes are more susceptible to bias from the frequent location of sites near urban centers. *Norris and Wild* [2009] calculate East China clear-sky SSR trends using the same method as *Allen et al.* [2013], but with a more densely sampled set of observation sites with greater representation of interior China, and find different trend values, suggesting a sensitivity to the sampling choices made. We have chosen, therefore, to focus primarily on physical analysis of the model results, using observations primarily for context.

## 5. Conclusions

Our results demonstrate that it is possible to obtain SSR reductions over China that are comparable to observed trends via very different combinations of aerosol mechanisms, and that these reductions are strongly driven by increased aerosol absorption. Both the AM2.1 and AM3 AGCMs used in this study capture the decreasing trend in SSR over China from 1960 to the mid-2000s, though AM2.1's trend is larger than AM3's. The two models contain large, virtually identical increases in absorption over this period, however, despite having significantly different aerosol treatments, including differences in aerosol interactivity, mixing state, and column burden.

Our analysis using the models' standalone radiation module reveals that the difference in mixing state and aerosol amount between the two models act on the absorption and SSR values in opposing directions, resulting in a compensation of effects that largely explains the similarity in absorption increase between the two models. AM3's internal mixing increases the absorption produced by its smaller change in black carbon column burden, while AM2.1 compensates for the smaller normalized absorption induced by its external mixing scheme with a change in black carbon column burden that is a factor of 2 larger than AM3's. The hygroscopic growth of internally mixed aerosol in AM3 also acts to enhance the absorption that the model's aerosol population produces.

The framework developed in this paper can be extended to study the impact of many other aerosol characteristics that may be important for determining the relative contribution of absorption to aerosol-driven solar dimming. We briefly discuss the impact of the seasonality of the aerosol concentrations in the two models, but greater insight could be achieved via in-depth standalone radiative transfer calculations. Given the climate impacts of aerosol absorption and the sensitivity of that absorption to subtle changes in aerosol characteristics discussed in this study, in-depth mechanistic analyses such as those contained in this paper will be vital to constraining the climate response to aerosol-driven solar dimming. In addition to the single variable dependencies discussed here, cross-correlations between different aerosol characteristics may also exist. For example, seasonal and vertical variations in relative humidity may lead to stronger hygroscopic growth depending on the seasonality and vertical distribution of the aerosols. The standalone radiative transfer calculation framework developed in this paper provides an ideal tool for analyzing these effects in future studies.

This work highlights the important role that aerosol absorption plays in driving solar dimming over East Asia, especially in the more recent incarnation of the GFDL model. AM3's aerosol treatment contains several advances in the complexity of its aerosol representation, and much of its aerosol treatment is considered to be more physically realistic than AM2.1's [*Donner et al.*, 2011]. The particularly strong contribution of absorption to the dimming trend produced by AM3, therefore, has many important implications for the climate response that can be expected from solar dimming over East Asia, especially as aerosol emissions evolve in the future. Given the strong regional impacts of the surface-atmosphere radiation dipole that aerosol absorption can impose [*Ramanathan et al.*, 2001], it will be critical the establish greater confidence in the relative contribution of absorption to solar dimming values.

**Acknowledgments.** The authors thanks Paul Ginoux and Stefan Fueglistaler for comments during early stages of the study. Geeta G. Persad is supported by the National Science Foundation Graduate Research Fellowship under grant DGE 1148900.

## References

Ackerman, A. S. (2000), Reduction of tropical cloudiness by soot, *Science*, *288*(5468), 1042–1047, doi:10.1126/science.288.5468.1042.

Ackerman, T. P., and O. B. Toon (1981), Absorption of visible radiation in atmosphere containing mixtures of absorbing and nonabsorbing particles, *Applied Optics*, *20*(20), 3661–3667, doi:10.1364/AO.20.003661.

Allen, R. J., J. R. Norris, and M. Wild (2013), Evaluation of multidecadal variability in CMIP5 surface solar radiation and inferred underestimation of aerosol direct effects

505 over europe, china, japan, and india, *Journal of Geophysical Research: Atmospheres*,
506 pp. n/a–n/a, doi:10.1002/jgrd.50426.

507 Andreae, M. O., R. J. Charlson, F. Bruynseels, H. Storms, R. V. Grieken, and W. Maen-
508 haut (1986), Internal mixture of sea salt, silicates, and excess sulfate in marine aerosols,
509 *Science*, *232*(4758), 1620–1623, doi:10.1126/science.232.4758.1620, PMID: 17812139.

510 Andrews, T., P. M. Forster, and J. M. Gregory (2009), A surface energy perspective on
511 climate change, *Journal of Climate*, *22*(10), 2557–2570, doi:10.1175/2008JCLI2759.1.

512 Bollasina, M. A., Y. Ming, and V. Ramaswamy (2011), Anthropogenic aerosols and
513 the weakening of the south asian summer monsoon, *Science*, *334*(6055), 502–505, doi:
514 10.1126/science.1204994.

515 Bond, T. C., et al. (2013), Bounding the role of black carbon in the climate system: A
516 scientific assessment, *Journal of Geophysical Research: Atmospheres*, *118*(11), 5380–
517 5552, doi:10.1002/jgrd.50171.

518 Charlson, R. J., J. Langner, H. Rodhe, C. B. Leovy, and S. G. Warren (1991), Perturbation
519 of the northern hemisphere radiative balance by backscattering from anthropogenic
520 sulfate aerosols, *Tellus A*, *43*(4), 152–163, doi:10.1034/j.1600-0870.1991.00013.x.

521 Che, H. Z., G. Y. Shi, X. Y. Zhang, R. Arimoto, J. Q. Zhao, L. Xu, B. Wang, and
522 Z. H. Chen (2005), Analysis of 40 years of solar radiation data from china, 1961–2000,
523 *Geophysical Research Letters*, *32*(6), doi:10.1029/2004GL022322.

524 Chylek, P., and J. Wong (1995), Effect of absorbing aerosols on global radiation budget,
525 *Geophysical Research Letters*, *22*(8), 929–931, doi:10.1029/95GL00800.

526 Chylek, P., V. Ramaswamy, and R. J. Cheng (1984), Effect of graphitic carbon on
527 the albedo of clouds, *Journal of the Atmospheric Sciences*, *41*(21), 3076–3084, doi:

10.1175/1520-0469(1984)041¡3076:EOGCOT¿2.0.CO;2.

Cooke, W. F., C. Liousse, H. Cachier, and J. Feichter (1999), Construction of a 1 ° 1 ° fossil fuel emission data set for carbonaceous aerosol and implementation and radiative impact in the ECHAM4 model, *Journal of Geophysical Research: Atmospheres*, *104*(D18), 22,137–22,162, doi:10.1029/1999JD900187.

Danielson, R. E., D. R. Moore, and H. C. van de Hulst (1969), The transfer of visible radiation through clouds, *Journal of the Atmospheric Sciences*, *26*(5), 1078–1087, doi:10.1175/1520-0469(1969)026¡1078:TTOVRT¿2.0.CO;2.

Donner, L. J., et al. (2011), The dynamical core, physical parameterizations, and basic simulation characteristics of the atmospheric component AM3 of the GFDL global coupled model CM3, *Journal of Climate*, *24*(13), 3484–3519, doi:10.1175/2011JCLI3955.1.

Dwyer, J. G., J. R. Norris, and C. Ruckstuhl (2010), Do climate models reproduce observed solar dimming and brightening over china and japan?, *Journal of Geophysical Research*, *115*(D7), D00K08, doi:10.1029/2009JD012945.

Folini, D., and M. Wild (2011), Aerosol emissions and dimming/brightening in europe: Sensitivity studies with ECHAM5-HAM, *Journal of Geophysical Research*, *116*(D21), doi:10.1029/2011JD016227.

Freidenreich, S. M., and V. Ramaswamy (2011), Analysis of the biases in the downward shortwave surface flux in the GFDL CM2.1 general circulation model, *Journal of Geophysical Research: Atmospheres*, *116*(D8), n/a–n/a, doi:10.1029/2010JD014930.

Fröhlich, C., and J. Lean (1998), The sun's total irradiance: Cycles, trends and related climate change uncertainties since 1976, *Geophysical Research Letters*, *25*(23), 4377–4380, doi:10.1029/1998GL900157.

Ginoux, P., L. W. Horowitz, V. Ramaswamy, I. V. Geogdzhayev, B. N. Holben, G. Stenchikov, and X. Tie (2006), Evaluation of aerosol distribution and optical depth in the geophysical fluid dynamics laboratory coupled model CM2.1 for present climate, *Journal of Geophysical Research: Atmospheres*, *111*(D22), doi:10.1029/2005JD006707.

Haywood, J. M., and V. Ramaswamy (1998), Global sensitivity studies of the direct radiative forcing due to anthropogenic sulfate and black carbon aerosols, *Journal of Geophysical Research: Atmospheres*, *103*(D6), 6043–6058, doi:10.1029/97JD03426.

Haywood, J. M., V. Ramaswamy, and B. J. Soden (1999), Tropospheric aerosol climate forcing in clear-sky satellite observations over the oceans, *Science*, *283*(5406), 1299–1303, doi:10.1126/science.283.5406.1299, PMID: 10037595.

Horowitz, L. W., et al. (2003), A global simulation of tropospheric ozone and related tracers: Description and evaluation of MOZART, version 2: MOZART-2 DESCRIPTION AND EVALUATION, *Journal of Geophysical Research: Atmospheres*, *108*(D24), 2156–2202, doi:10.1029/2002JD002853.

Jacobson, M. Z. (2000), A physically-based treatment of elemental carbon optics: Implications for global direct forcing of aerosols, *Geophysical Research Letters*, *27*(2), 217–220, doi:10.1029/1999GL010968.

Jacobson, M. Z., et al. (2001), Strong radiative heating due to the mixing state of black carbon in atmospheric aerosols, *Nature*, *409*(6821), 695–697.

Kassianov, E., J. Barnard, M. Pekour, L. K. Berg, J. Michalsky, K. Lantz, and G. Hodges (2013), Do diurnal aerosol changes affect daily average radiative forcing?, *Geophysical Research Letters*, *40*(12), 3265–3269, doi:10.1002/grl.50567.

573 Kaufman, Y. J. (1997), The effect of smoke particles on clouds and climate forcing, *Sci-*
574 *ence*, *277*(5332), 1636–1639, doi:10.1126/science.277.5332.1636.
575 Klein, S. A., Y. Zhang, M. D. Zelinka, R. Pincus, J. Boyle, and P. J. Gleckler (2013),
576 Are climate model simulations of clouds improving? an evaluation using the ISCCP
577 simulator, *Journal of Geophysical Research: Atmospheres*, *118*(3), 1329–1342, doi:
578 10.1002/jgrd.50141.
579 Koch, D., and A. D. Del Genio (2010), Black carbon semi-direct effects on cloud cover:
580 review and synthesis, *Atmospheric Chemistry and Physics*, *10*(16), 7685–7696, doi:
581 10.5194/acp-10-7685-2010.
582 Koch, D., et al. (2009), Evaluation of black carbon estimations in global aerosol models,
583 *Atmos. Chem. Phys.*, *9*(22), 9001–9026, doi:10.5194/acp-9-9001-2009.
584 Koffi, B., et al. (2012), Application of the CALIOP layer product to evaluate the vertical
585 distribution of aerosols estimated by global models: AeroCom phase I results, *Journal*
586 *of Geophysical Research: Atmospheres*, *117*(D10), 201–227, doi:10.1029/2011JD016858.
587 Lamarque, J.-F., et al. (2010), Historical (1850–2000) gridded anthropogenic and biomass
588 burning emissions of reactive gases and aerosols: methodology and application, *Atmos.*
589 *Chem. Phys.*, *10*(15), 7017–7039, doi:10.5194/acp-10-7017-2010.
590 Liao, H., and J. H. Seinfeld (2005), Global impacts of gas-phase chemistry-aerosol in-
591 teractions on direct radiative forcing by anthropogenic aerosols and ozone, *Journal of*
592 *Geophysical Research: Atmospheres*, *110*(D18), doi:10.1029/2005JD005907.
593 Lohmann, U., and J. Feichter (2001), Can the direct and semi-direct aerosol effect compete
594 with the indirect effect on a global scale?, *Geophysical Research Letters*, *28*(1), 159–161.

595 Ming, Y., V. Ramaswamy, and G. Persad (2010), Two opposing effects of absorb-
596 ing aerosols on global-mean precipitation, *Geophysical Research Letters*, *37*(13), doi:
597 10.1029/2010GL042895.

598 Nazarenko, L., and S. Menon (2005), Varying trends in surface energy fluxes and associ-
599 ated climate between 1960 and 2002 based on transient climate simulations, *Geophysical*
600 *Research Letters*, *32*(22), doi:10.1029/2005GL024089.

601 Norris, J. R., and M. Wild (2007), Trends in aerosol radiative effects over europe in-
602 ferred from observed cloud cover, solar "dimming," and solar "brightening", *Journal of*
603 *Geophysical Research*, *112*(D8), doi:10.1029/2006JD007794.

604 Norris, J. R., and M. Wild (2009), Trends in aerosol radiative effects over china and japan
605 inferred from observed cloud cover, solar "dimming," and solar "brightening", *Journal*
606 *of Geophysical Research*, *114*(D10), D00D15, doi:10.1029/2008JD011378.

607 Ocko, I. B., V. Ramaswamy, P. Ginoux, Y. Ming, and L. W. Horowitz (2012), Sensitivity
608 of scattering and absorbing aerosol direct radiative forcing to physical climate factors,
609 *Journal of Geophysical Research: Atmospheres*, *117*(D20), doi:10.1029/2012JD018019.

610 Olivier, J. (1996), Description of the edgar version 2.0: A set of global emission inventories
611 of greenhouse gases and ozone-depleting substances for all anthropogenic and most
612 natural sources on a per country basis and on 1x1 grid., *Tech. Rep. Rep. 771060 002,*
613 *TNO-MEP Rep. R96/119*, National Institute of Public Health and the Environment
614 (RIVM).

615 Persad, G. G., Y. Ming, and V. Ramaswamy (2012), Tropical tropospheric-only responses
616 to absorbing aerosols, *Journal of Climate*, *25*(7), 2471–2480, doi:10.1175/JCLI-D-11-
617 00122.1.

Pósfai, M., J. R. Anderson, P. R. Buseck, and H. Sievering (1999), Soot and sulfate aerosol particles in the remote marine troposphere, *Journal of Geophysical Research: Atmospheres*, *104*(D17), 21,685–21,693, doi:10.1029/1999JD900208.

Qian, Y., D. P. Kaiser, L. R. Leung, and M. Xu (2006), More frequent cloud-free sky and less surface solar radiation in china from 1955 to 2000, *Geophysical Research Letters*, *33*(1), n/a–n/a, doi:10.1029/2005GL024586.

Qian, Y., W. Wang, L. R. Leung, and D. P. Kaiser (2007), Variability of solar radiation under cloud-free skies in china: The role of aerosols, *Geophysical Research Letters*, *34*(12), doi:10.1029/2006GL028800.

Ramanathan, V., and G. Carmichael (2008), Global and regional climate changes due to black carbon, *Nature Geoscience*, *1*(4), 221–227.

Ramanathan, V., P. J. Crutzen, J. T. Kiehl, and D. Rosenfeld (2001), Aerosols, climate, and the hydrological cycle, *Science*, *294*(5549), 2119–2124, doi:10.1126/science.1064034.

Ramanathan, V., et al. (2005), Atmospheric brown clouds: Impacts on south asian climate and hydrological cycle, *Proceedings of the National Academy of Sciences of the United States of America*, *102*(15), 5326–5333, doi:10.1073/pnas.0500656102, PMID: 15749818.

Reichler, T., and J. Kim (2008), How well do coupled models simulate today's climate?, *Bulletin of the American Meteorological Society*, *89*(3), 303–311, doi:10.1175/BAMS-89-3-303.

Ruckstuhl, C., and J. R. Norris (2009), How do aerosol histories affect solar "dimming" and "brightening" over europe?: IPCC-AR4 models versus observations, *Journal of Geophysical Research*, *114*, doi:10.1029/2008JD011066.

Sato, M., J. Hansen, D. Koch, A. Lacis, R. Ruedy, O. Dubovik, B. Holben, M. Chin, and T. Novakov (2003), Global atmospheric black carbon inferred from AERONET, *Proceedings of the National Academy of Sciences*, *100*(11), 6319–6324, doi:10.1073/pnas.0731897100, PMID: 12746494.

Shi, G.-Y., T. Hayasaka, A. Ohmura, Z.-H. Chen, B. Wang, J.-Q. Zhao, H.-Z. Che, and L. Xu (2008), Data quality assessment and the long-term trend of ground solar radiation in china, *Journal of Applied Meteorology and Climatology*, *47*(4), 1006–1016, doi:10.1175/2007JAMC1493.1.

Stier, P., J. H. Seinfeld, S. Kinne, and O. Boucher (2007), Aerosol absorption and radiative forcing, *Atmospheric Chemistry and Physics*, *7*(19), 5237–5261.

Streets, D. G., Y. Wu, and M. Chin (2006), Two-decadal aerosol trends as a likely explanation of the global dimming/brightening transition, *Geophysical Research Letters*, *33*(15), doi:10.1029/2006GL026471.

Streets, D. G., F. Yan, M. Chin, T. Diehl, N. Mahowald, M. Schultz, M. Wild, Y. Wu, and C. Yu (2009), Anthropogenic and natural contributions to regional trends in aerosol optical depth, 1980–2006, *Journal of Geophysical Research: Atmospheres*, *114*(D10), doi:10.1029/2008JD011624.

Tang, W., K. Yang, J. He, and J. Qin (2010), Quality control and estimation of global solar radiation in china, *Solar Energy*, *84*(3), 466–475, doi:10.1016/j.solener.2010.01.006.

Tang, W.-J., K. Yang, J. Qin, C. C. K. Cheng, and J. He (2011), Solar radiation trend across china in recent decades: a revisit with quality-controlled data, *Atmos. Chem. Phys.*, *11*(1), 393–406, doi:10.5194/acp-11-393-2011.

**Table 1.** A summary of salient differences in aerosol treatment between AM2.1 and AM3.

| **Feature** | **AM2.1** [*GAMDT*, 2004] | **AM3** [*Donner et al.*, 2011] |
|---|---|---|
| Emissions | *Olivier* [1996];*Cooke et al.* [1999] | *Lamarque et al.* [2010] |
| Optical Properties | *Haywood and Ramaswamy* [1998]; *Haywood et al.* [1999] | *Haywood and Ramaswamy* [1998]; *Haywood et al.* [1999] |
| Interactivity | No<br>Prescribed from MOZART [*Horowitz et al.*, 2003] | Yes |
| Mixing State | All external | BC/Sulfate internally mixed<br>All else externally mixed |
| Hygroscopicity | Sulfate: to 100% RH<br>BC: no | Sulfate: to 97% RH<br>BC: when mixed |

The GFDL Global Atmospheric Model Development Team (*GAMDT*) (2004), The new GFDL global atmosphere and land model AM2–LM2: evaluation with prescribed SST simulations, *Journal of Climate*, *17*(24), 4641–4673, doi:10.1175/JCLI-3223.1.

Twomey, S. (1974), Pollution and the planetary albedo, *Atmospheric Environment (1967)*, *8*(12), 1251–1256.

Wild, M. (1997), *The Heat Balance of the Earth in GCM Simulations of Present and Future Climates*, Geographisches Institut Eidgenössische Technische Hochschule.

Wild, M. (2009), Global dimming and brightening: A review, *Journal of Geophysical Research*, *114*, doi:10.1029/2008JD011470.

Wild, M. (2012), Enlightening global dimming and brightening, *Bulletin of the American Meteorological Society*, *93*(1), 27–37, doi:10.1175/BAMS-D-11-00074.1.

Wild, M., and E. Schmucki (2010), Assessment of global dimming and brightening in IPCC-AR4/CMIP3 models and ERA40, *Climate Dynamics*, *37*(7-8), 1671–1688, doi:10.1007/s00382-010-0939-3.

Willson, R. C., and A. V. Mordvinov (2003), Secular total solar irradiance trend during solar cycles 21–23, *Geophysical Research Letters*, *30*(5), doi:10.1029/2002GL016038.

**Table 2.** A summary of the standalone radiation radiative transfer calculation results. SSR and absorption values shown are for 1990 aerosol concentrations minus 1970 aerosol concentrations. The '_nohygro' refers to the versions of each experiment with hygroscopic growth disabled.

| | AM3_IM | AM3_EM | AM2_IM | AM2_EM |
|---|---|---|---|---|
| Run Description | AM3 aerosol climatology with internal mixing (baseline) | AM3 aerosol climatology with external mixing | AM2.1 aerosol climatology with internal mixing | AM2.1 aerosol climatology with external mixing (baseline) |
| SSR ($Wm^{-2}$) | -6.9 | -5.6 | -10.3 | -8.5 |
| _nohygro | -5.2 | -4.1 | -8.1 | -6.3 |
| Absorption ($Wm^{-2}$) | 4.3 | 2.2 | 6.5 | 3.1 |
| _nohygro | 3.8 | 2.3 | 6.0 | 3.3 |
| Norm. Abs. ($MWkg^{-1}$) | 8.0 | 4.1 | 7.2 | 3.5 |

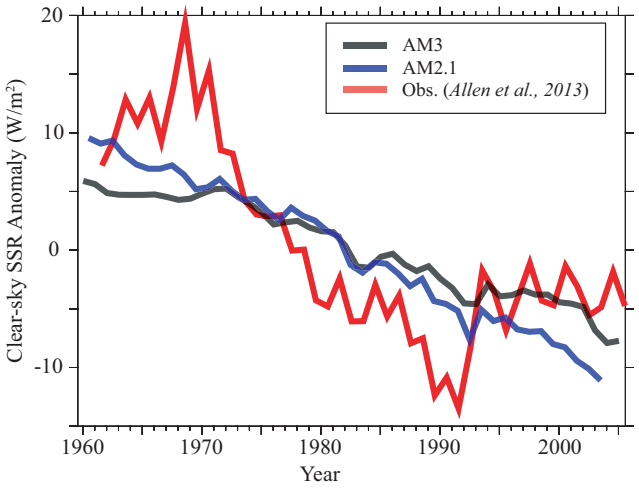


**Figure 1.** Clear-sky surface solar radiation (SSR) anomalies in $Wm^{-2}$ in AM3 (black), AM2.1 (blue), and the observational estimate from *Allen et al.* [2013] (red).

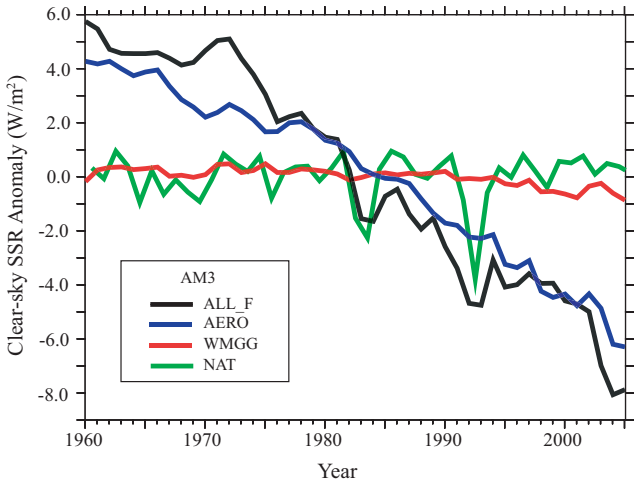


**Figure 2.** Clear-sky SSR anomaly in $Wm^{-2}$ is shown for various AM3 attribution runs. The natural forcing (NAT, red) and greenhouse gas only (WMGG, green) runs show no significant trend, while the aerosol-only (AERO, blue) run explains the majority of the trend seen in the all-forcing run (ALL_F, black)

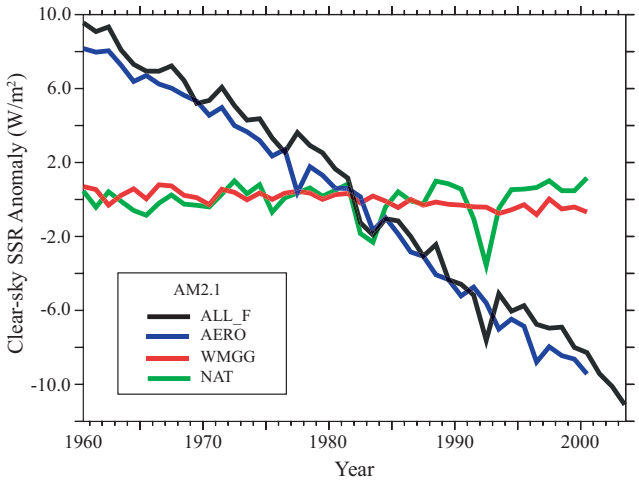


**Figure 3.** Same as for Figure 2, but for AM2.1.

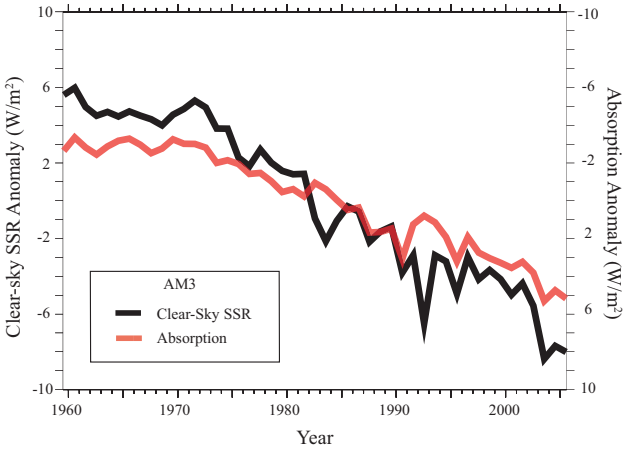


**Figure 4.** The clear-sky SSR (left axis, black) and atmospheric absorption (right axis, red) anomalies are shown for AM3. Increasing absorption accounts for approximately one half of the decrease in SSR.

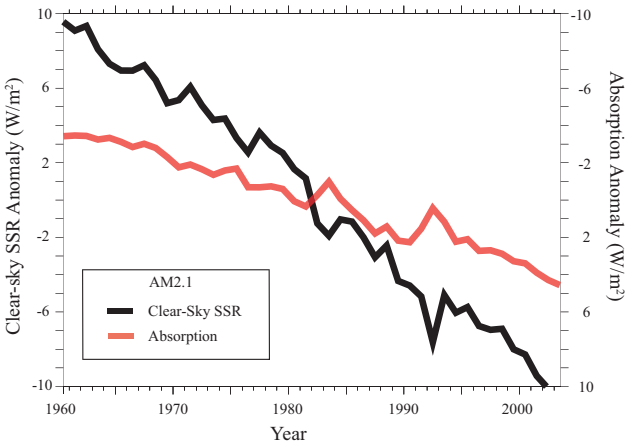


**Figure 5.** Same as for Figure 4, but for AM2.1. Increasing absorption accounts for approximately one third of the decrease in SSR.

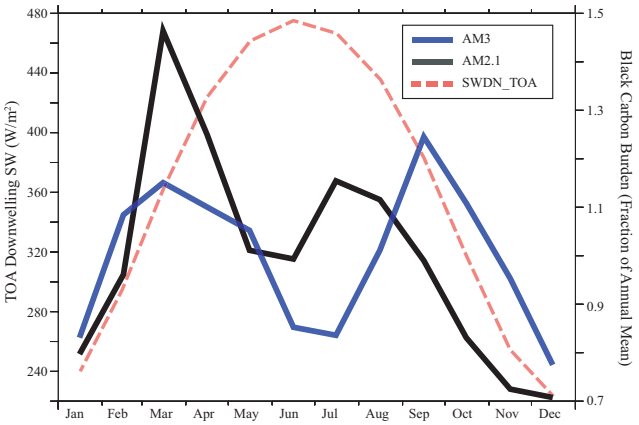


**Figure 6.** Seasonal variation of black carbon column burden is shown for AM2.1 (black) and AM3 (blue) normalized by each model's annual mean value. Also shown is the top-of-atmosphere (TOA) downwelling shortwave radiation (red) over East China in $Wm^{-2}$ for reference. The two models have significantly different black carbon seasonalities, which lead to different temporal correlations with the downwelling radiation.